

Variation in b-value of caldera earthquakes during recent activity of the Bárðarbunga Volcano in Iceland

Magnús Pálsson¹, Páll Einarsson² and Birgir Hrafnkelsson¹

¹Department of Mathematics, Faculty of Physical Sciences,

School of Engineering and Natural Sciences, University of Iceland, Dunhagi 5, 107 Reykjavík

²Institute of Earth Sciences, University of Iceland, Sturlugata 7, 101 Reykjavík; palli@hi.is

<https://doi.org/10.33799/jokull2019.69.071>

Abstract — *The magnitude distribution of caldera earthquakes in the subglacial Bárðarbunga volcano in Central Iceland, characterized by the b-value, shows a systematic variation that is consistent with stress changes anticipated in the roof of an inflating magma chamber beneath the caldera. The b-value was 0.83 prior to the rupture of the chamber in August 2014 when a dike propagated laterally from the volcano to feed the eruption in Holuhraun. The b-value was relatively high following the collapse of the caldera, reflecting low stress in the magma chamber roof. Half a year later a decrease was observed in the b-value, concurrent with an increase in the seismicity, consistent with indications of recharging of the volcano magma chamber. The magnitude distribution was anomalous during the slow collapse of the caldera in association with the eruption. During this period the earthquake sequence appeared to consist of two populations, only one of which followed the conventional Gutenberg-Richter distribution. For a subglacial volcano, where geodetic methods are difficult to implement, the b-value of caldera earthquakes provides an important additional parameter for the monitoring of magma pressure variations.*

Key points

The Bárðarbunga volcano at the center of the Iceland Hotspot is re-inflating following a major eruption and caldera collapse in 2014–2015.

The magnitude distribution of caldera earthquakes is consistent with increasing stress in the caldera region.

The b-value of the caldera earthquakes provides an addition to the arsenal of useful monitoring parameters for this remote sub-glacial volcano.

INTRODUCTION

The Gutenberg-Richter relation $\log N = a - bM$ is one way of quantifying an earthquake sequence. Here N is the number of earthquakes of magnitude M and larger, a and b are constants. The slope of this linear relationship, the b-value, describes the relative frequency of small events versus that of large events and a is the logarithm of the number of earthquakes of magnitude 0 and larger. For ordinary tectonic areas the value of b is close to 1 and shows little change. For some areas, however, volcanic areas in particular, the b-value

is significantly different from 1. The spreading segments of mid-oceanic ridges, e.g., have consistently higher b-values, as high as 2.6 (Sykes, 1970; Einarsson, 1986).

It is generally accepted, following Scholz (1968) and Wyss (1973), that the b-value is inversely dependent on the stress level in the seismically active volume. High stress level over a large area favors large events over small events, hence a low b-value. High b-value is expected in areas of low stress and heterogeneous crust, where small earthquakes are favored. This has led to numerous studies where the objec-

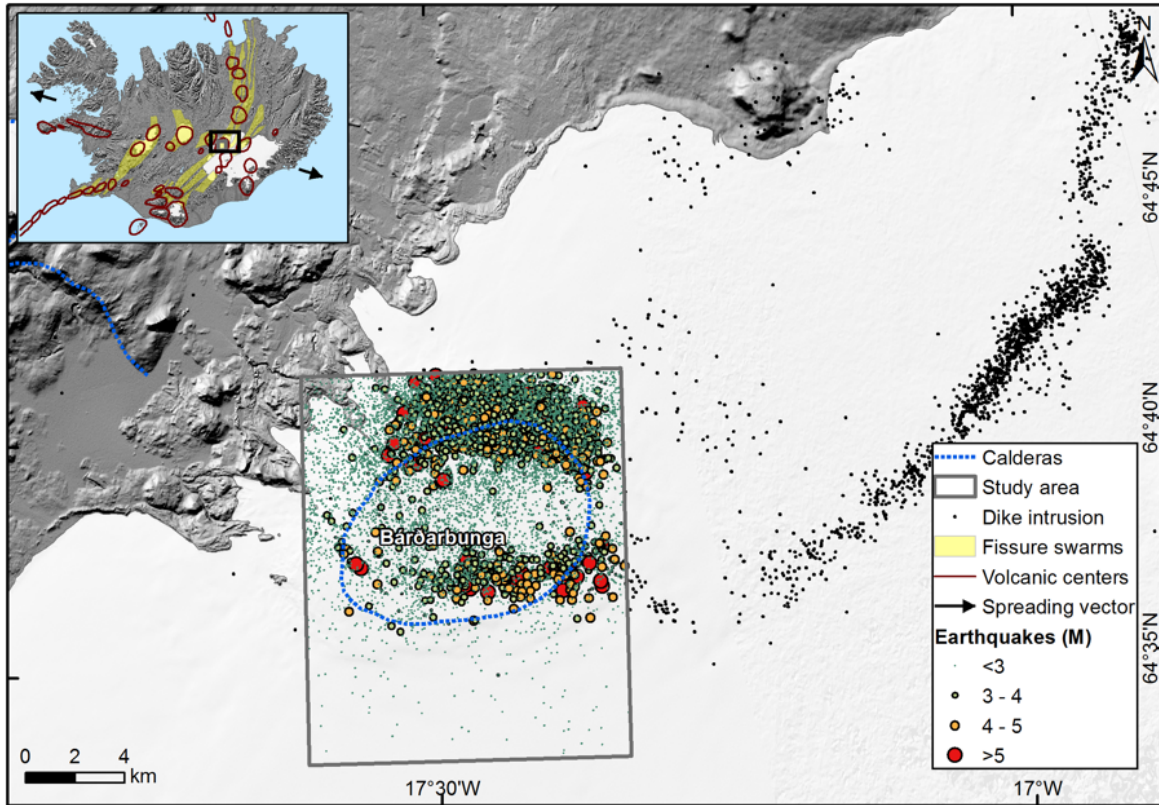


Figure 1. Map of the study area around the Bárðarbunga volcano, showing epicenters of the period of unrest, 2010–2017. The inset map shows the volcanic systems of Iceland according to Einarsson and Sæmundsson (1987) as modified by Hjartardóttir *et al.* (2016a). – *Kort af Bárðarbungu og rannsóknarsvæðinu umhverfis hana. Punktar sýna skjálftamiðjur jarðskjálfta sem urðu á umbrotasvæðinu 2010–2017. Innfellda kortið sýnir eldstöðvarkerfi á Íslandi.*

tive is to use the b-value of a region for monitoring purposes as a proxy for stress (see e.g., Kulhanek, 2005 for summary). Furthermore, consistently high b-values are expected in crustal volumes where the strength is low, as for example in volcanic areas where magmatic heat has an effect on rock properties (e.g., Wiemer *et al.*, 1998; Riedel *et al.*, 2003) preventing large earthquakes. A comprehensive review of previous investigations into the spatial and temporal variations of b-value suggests that they are most plausibly linked with changes in effective stress (El-Isa and Eaton, 2014).

Three volcanoes in Iceland show an unusually continuous and persistent seismic activity, Hengill, Katla, and Bárðarbunga (Einarsson, 1991a). The seismic activity of the Bárðarbunga volcano offers a good opportunity to study the frequency-magnitude distribution of earthquakes in a relatively isolated environment (Figure 1) and relate it to tectono-magmatic events that have taken place there in recent years. This volcano has been going through phases of large earthquakes 1974 to 1996 (Einarsson *et al.*, 1997; Bjarnason, 2014), relative quiescence 1996 to 2002, increasing seismicity 2002 to 2014 (Jakobsdóttir, 2008),

caldera collapse 2014 to 2015 (Gudmundsson *et al.*, 2016), and re-inflation of the volcano, 2015 to present (Sigmundsson *et al.*, 2018). In this paper we test the proposition that this last change is in some way reflected in a changing *b*-value.

RECENT ACTIVITY OF THE BÁRÐARBUNGA VOLCANO

Bárðarbunga is located in Central Iceland, near the center of the Iceland Hotspot (Wolfe *et al.*, 1997), at a triple junction where three branches of the Icelandic plate boundary meet (e.g. Einarsson, 2008). Due to its remoteness Bárðarbunga was not discovered as an active volcano until 1973 when the first satellite images of Iceland became available (Thorarinnsson *et al.*, 1973) and a caldera structure was evident beneath the Vatnajökull glacier. The caldera was found to be the central element in an extensive volcanic system, which fissure swarms extend 100 km to the SW and at least 60 km to the NE (e.g., Sæmundsson, 1978; Einarsson and Sæmundsson, 1987; Hjartardóttir *et al.*, 2016a). The caldera is about 700 m deep and filled to the rim by glacier ice (Björnsson, 1988). The caldera and the NE fissure swarm were found to be seismically quite active (Björnsson and Einarsson, 1990; Einarsson, 1986, 1991a). Studies of tephra deposits revealed large historic and prehistoric fissure eruptions in the fissure swarms, the SW swarm in particular (Larsen, 1984). The largest known is the Thjórsá Lava of South Iceland, a 20 km³ volume lava flow emplaced around 8000 a (e.g., Hjartarson, 1994). Lava flows from the Bárðarbunga volcanic system have reached the south shore of Iceland and almost to the north shore as well (Hjartarson and Sæmundsson, 2014; Svavarsdóttir *et al.*, 2017). No other Icelandic volcano has spread lavas as widely as this. Large recent eruptions include the Vatnaöldur eruption of ~870, Veiðivötn eruption ~1480, and Tröllahraun eruption of 1864–1866 (Larsen, 1984), all within the SW fissure swarm, a part of the Eastern Volcanic Zone in South Iceland.

Earthquake monitoring of the Bárðarbunga area goes as far back as 1975, when the first stations in a country-wide seismic network were installed in North

Iceland (Einarsson and Björnsson, 1987) and epicentral locations became sufficiently accurate to separate the activity of different volcanoes in the area. The accuracy increased significantly in 1985 when telemetered stations were installed in Central Iceland. A new digital network replaced these analog stations in 1990–1994, again increasing the detectability of events in Central Iceland. All this time it was clear that the caldera region of Bárðarbunga was seismically active (e.g., Björnsson and Einarsson, 1990; Einarsson, 1991a; Jakobsdóttir, 2008) and was going through different phases of activity. The period 1974–1996 was particularly active. About 15 earthquakes of magnitude 5 and larger occurred at regular intervals during this time but had been unknown before that. Their focal mechanisms had a large component of reverse faulting, interpreted by Einarsson (1986) to be the result of slow deflation of the volcano. Other authors considered this to be due to inflation of the volcano (Zobin, 1999; Nettles and Ekström, 1998; Bjarnason, 2014). This activity ended abruptly in 1996 when the Gjalp eruption occurred, a fissure eruption about 15 km south of Bárðarbunga (Einarsson *et al.*, 1997; Gudmundsson *et al.*, 1997). The activity remained relatively low for several years but began to increase slowly in 2002 (Jakobsdóttir, 2008).

A new phase began in August 2014 when a dike started propagating away from the volcano and the caldera floor subsided. The dike propagated 48 km laterally for two weeks, accompanied by earthquake activity and graben formation until a lava eruption began from its distal end (Sigmundsson *et al.*, 2015; Hjartardóttir *et al.*, 2016b; Ágústsdóttir *et al.*, 2019). The eruption continued for six months and produced 1.4 km³ of lava. This was accompanied by a slow collapse of the Bárðarbunga caldera, a total of 65 m, and a series of earthquakes there, at least 70 of which were of magnitude 5 and larger (Gudmundsson *et al.*, 2016). Following the end of the eruption the earthquake activity became relatively low for several months. But in the fall of 2015 the earthquake activity in the caldera increased again and continued at a constant rate for about two years, then slowly decreasing. The largest events of this last period exceeded magnitude 4, but were smaller than 5.

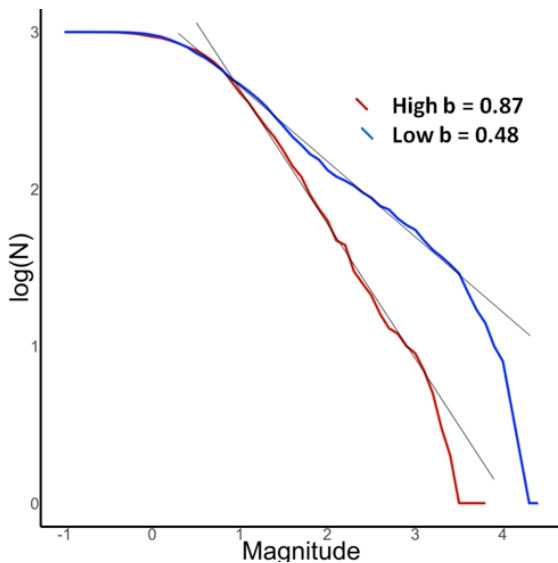


Figure 2. $\log N$ as a function of M for two different periods. The red curve shows the period immediately following the eruption and the caldera collapse, April 1 – December 23, 2015. The b -value is 0.87. The blue curve is for the period October 29, 2016 – June 4, 2017 and shows an anomalously low b -value, 0.48. Both data sets contain 1000 earthquakes. Lines with a slope of -0.48 and -0.87 are shown for comparison. The 95% confidence interval of these values is ± 0.03 and ± 0.05 , respectively.

– *Stærðardreifing jarðskjálfta á tveimur mismunandi tímabilum. Rauða línuritið gildir fyrir tímabilið rétt á eftir að gosinu lauk í Holuhrauni og hrun Bárðarbunguöskjunnar hætti, 1. apríl – 23. desember 2015. Gildið á b er 0,87. Bláa línuritið sýnir dreifinguna á tímabilinu 29. október 2016 – 4. júní 2017. Gildið á b er 0,48. Á báðum tímabilunum mældust 1000 skjálftar. Línur með hallatölunum $-0,87$ og $-0,48$ eru sýndar til viðmiðunar. 95% öryggismörk fyrir hallatölurnar eru $\pm 0,05$ og $\pm 0,03$.*

METHODS

The earthquake data were taken from the online records of the Icelandic Meteorological Office, available on their website. Two representative samples of magnitude-frequency distributions are shown in Figure 2. Both contain 1000 events. The curves show a familiar pattern of a linear relationship in the middle section and significant deviations from linearity at the low and high magnitude end of the curves. At the lower end the deviation is clearly caused by the incompleteness of the earthquake catalog. Small events are missing. The knee in the curve shows the limit of detection for the seismic network. At the high magnitude end the curve is determined by only few events, ten or less. These points have only a limited effect on the slope of the curve. We try to circumvent these irregularities by fitting the distribution curve by three line-segments. The b -value is taken to be given by the slope of the middle segment, that represents a large proportion of the data.

The R package “segmented” was used to fit a segmented linear regression model to the log of the cumulative distribution of earthquake magnitudes as

suggested by the Gutenberg-Richter relation. The package implements an iterative procedure described in Muggeo (2003). Three segments were used, with the slope of the central one giving the b -value. The package also supplies estimates for a 95% confidence interval for the slope. It should be noted that this estimate does not take into account the varying frequency of earthquakes, and with it the varying time period used for estimating the b -value. Further research is needed to determine how this affects the uncertainty.

When calculating a time series of b -values, a moving window with a fixed number of earthquakes was used, with the b -value being calculated at every stop. The amount of smoothing was controlled by the window size and by how far the window was moved after each iteration. The window size was chosen in an ad hoc way as being large enough to provide adequate smoothing to reveal underlying trends but no larger.

RESULTS

A preliminary inspection of the data set reveals large variations of the b -value with time. This is clearly seen in Figure 2, where the events of two different time slots are compared. Magnitude distribution is

shown for the period immediately following the collapse of the caldera, from April 1 to December 23, 2015. The seismic activity was low in the beginning but increased towards the autumn. The period contains 1000 events. The other curve shows the magnitude distribution in the period October 29, 2016, to June 4, 2017, also containing 1000 events. The figure show that the earthquakes during these periods follow the linear Gutenberg-Richter relationship quite well. The plots show similarity, a regular slope between magnitude 1 and 3 and a steeper curve above the knee at magnitude 3. Similar curves are found in various tectonic environments, showing lack of large events and therefore steepening of the curve towards higher magnitudes (see e.g., Einarsson, 1986). There is visible difference, however, between the *b*-values of the two curves, far exceeding the 95% confidence interval of the slope, ± 0.03 and ± 0.05 , respectively.

For comparison, the distribution curves for the collapse period are plotted in Figure 3, both for the number of events and the cumulative number, *N*. These plots show a very different behavior from that of the inflation period. The curve of cumulative frequency has two kinks, upwards at magnitude around

2.5 and downwards at magnitude 4. This is a very unusual behavior. A closer inspection of the frequency plot reveals that the first kink is due to an increase in the frequency of events of magnitude 4–5 compared to lower magnitude events. The earthquake population appears to be a sum of two populations, one following a power law according to Gutenberg-Richter, and the other with something resembling a normal distribution of magnitudes. A simulation of such a sum of distributions was attempted using the R functions `rexp()` and `rnorm()` with 80000 values from an exponential distribution with $\lambda = 1$ and 20000 values from a normal distribution with $\mu = 4$ and $\sigma = 0.5$. The simulated lists were then combined and a histogram produced (Figure 4). All values were chosen ad hoc to produce the desired qualitative result. The simulation does not include a dropoff in frequency for smaller earthquakes such as would be expected from measurement data, and is clearly seen in Figure 3. This simulation is not the only way to model the distribution, but it shows that such a simulation is possible. In particular, we stress that a simulation by two exponential distributions according to Gutenberg-Richter is not possible.

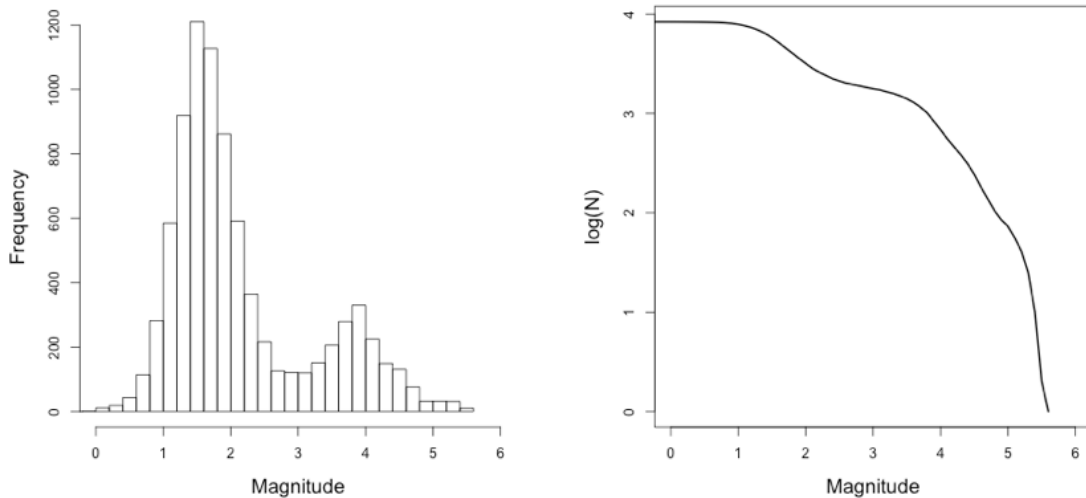


Figure 3. Magnitude distribution for the collapse period, August 16, 2014 to February 28, 2015, both frequency (left) and cumulative frequency (right), *N*, as a function of *M*. The clear increase in the frequency of earthquakes above magnitude 3.5 is anomalous. – *Stærðardreifing skjálfta fyrir hruntímabilið frá 16. ágúst 2014 til 28. febrúar 2015, bæði tíðni einstakra gilda og uppsafnaður fjöldi, sem fall af stærð *M*. Fjölgun skjálfta fyrir ofan stærðina 3,5 er mjög afbrigðileg.*

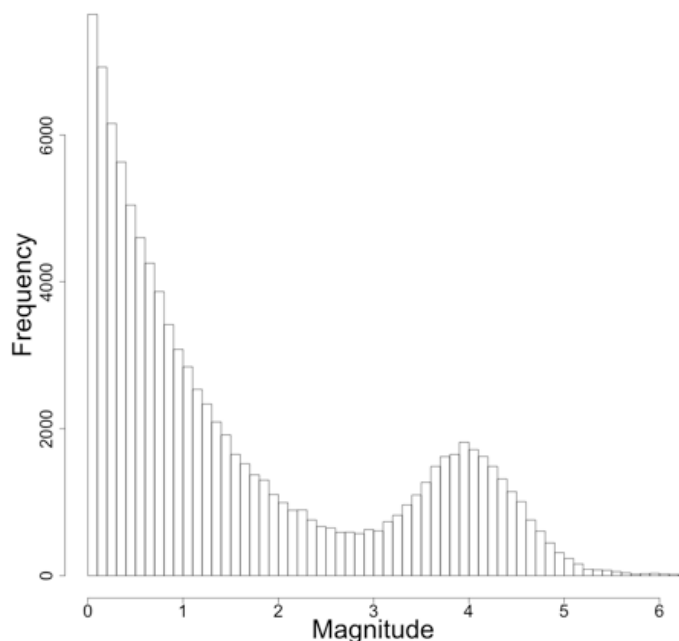


Figure 4. A simulation of the magnitude distribution of two earthquake populations, one with a conventional Gutenberg-Richter power law distribution, the other with a normal distribution. – *Hermun á stærðardreifingu þar sem saman fara tvö skjálftamengi. Annað fylgir hinu venjulega lögmáli Gutenbergs og Richters, hitt er normaldreift.*

The time variation of the b -value, as plotted in Figure 5, shows a systematic behavior. Before the eruption and collapse of the caldera the seismicity was moderate and the b -value was close to normal, 0.83 for the period 2010 to 2014. Low values are seen all through the collapse period, which is arguable because the distribution is not quite linear, see above. Immediately following the end of the eruption and collapse the seismic activity becomes low and the b -value increases back to normal values. As the seismic activity begins to increase in the fall of 2015 the b -value begins to decrease, and remains low at the time of writing (October 2019). The seismic activity reached a maximum in 2017–2018 and then began to decline slowly.

DISCUSSION

The b -values determined in this study are mostly within the range 0.4 to 1.4. Typical values for seismically active areas are around 1.0, and in volcanic areas the values are frequently higher (see e.g. Kulhanek, 2005). Such normal and higher values are found in our study only during the few months of 2015 immediately following the end of the Holuhraun eruption

when the stress in the caldera may be assumed to be low. At other times the values are between 0.4 and 0.5. Our abnormally low values are hard to explain. A large majority of the caldera earthquakes occurred along the northern and southern section of the caldera fault, as seen in Figure 1. Parts of the caldera ring-fault appear to have moved aseismically. The very low b -value may indicate that the stress is concentrated and very high on the seismically active section of the caldera fault.

The steepening of the frequency-magnitude curves towards higher magnitude, as seen in Figure 2, is a commonly observed phenomenon and we see this behavior in our whole data set. In a volcanic area this may be understood as a result of the finite extent of the stress field produced by the volcano. The source of the stress is in processes taking place in the root of the volcano, and the stress dies out rather quickly with distance from a point-like source. This limits the magnitude of earthquakes that can occur and the distribution curve becomes steep. Our three-segment fitting to the distribution was meant to take this effect into account.

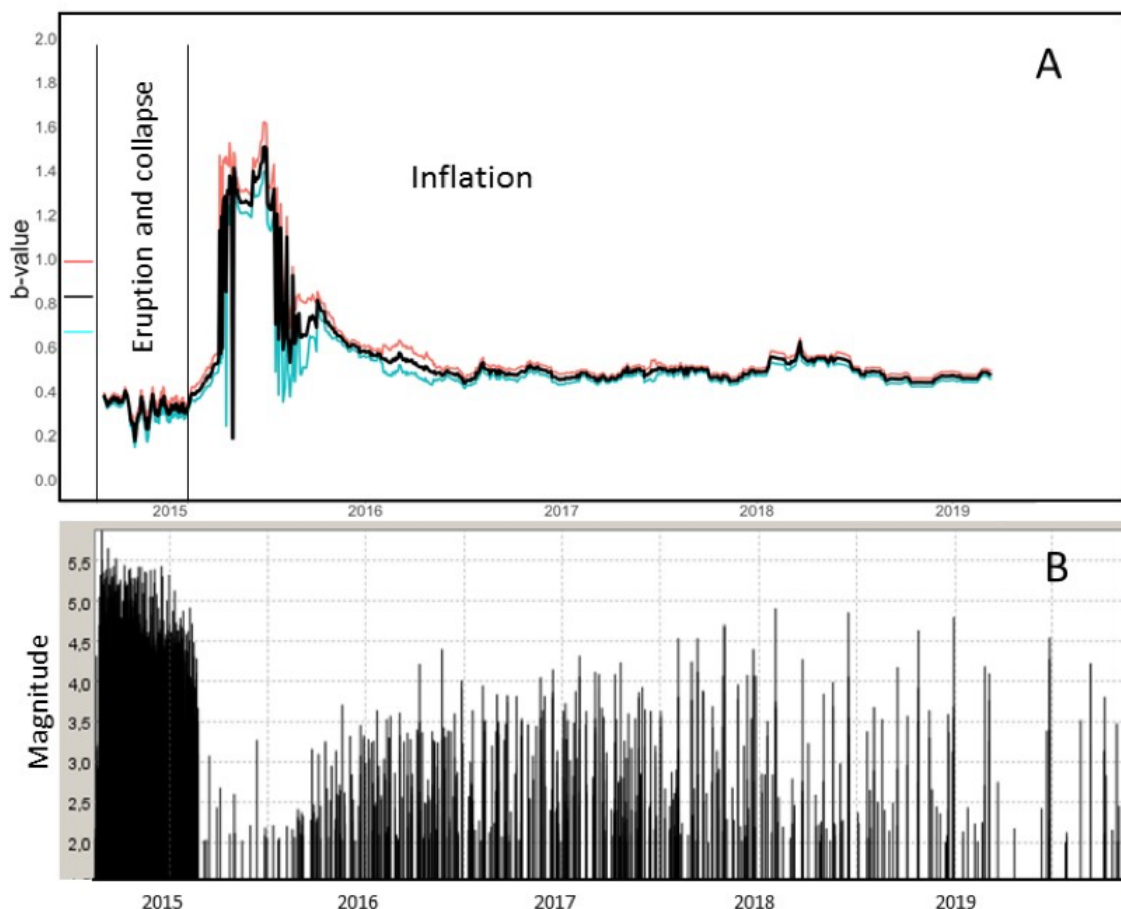


Figure 5. A) The b -value as a function of time during 2014–2019 for windows of 600 events. Red and blue curves give the 95% confidence interval. The dataline to the far left shows the b -value of the pre-eruption period beginning on Jan. 1, 2010, with 95% confidence interval. B) Magnitude of the caldera earthquakes as a function of time. Only events of magnitude 2 and larger are shown. – A) *Línurit sem sýnir b -gildi sem fall af tíma 2014–2019. Hvert gildi er reiknað fyrir 600 skjálfta úrtak. Rauða og bláa línan sýna 95% öryggismörk. Gildið lengst til vinstri sýnir b -gildið á tímabilinu frá 2010 og fram að gosi.* B) *Stærðir skjálfta í Bárðarbunguöskjunninni á sama tímakvarða. Aðeins skjálftar af stærðinni 2 og stærri eru sýndir.*

There is a pronounced difference between the earthquake population occurring during a collapse period of the volcano and the period when we infer inflation and uplift of the volcano is taking place. The maximum magnitude of inflation-related earthquakes appears to be below 5, whereas during the collapse period earthquakes exceeding magnitude 5 were common. In fact, they seem to form a special class of earthquakes with unusual magnitude distri-

bution. Similar difference was observed during the Krafla rifting episode of 1975–1984 in the Northern Volcanic Zone. Earthquakes during repeated inflation periods of Krafla volcano rarely exceeded magnitude 4, and the only caldera earthquakes larger than magnitude 5 occurred during the first and largest deflation event that had maximum deflation of 2 m (Einarsson, 1986; 1991b). Since the calderas of Krafla and Bárðarbunga are of similar dimensions it is tempting

to conclude that there may be a general relationship, that maximum magnitude is different for inflation and deflation of a caldera. In this light we may take the magnitude of the large earthquakes that took place at Bárðarbunga during the period 1974–1996 as indication of deflation of the volcano during that time (Einarsson, 1991a) rather than inflation as suggested by several authors (Zobin, 1999; Nettles and Ekström, 1998; Bjarnason, 2014).

The seismic efficiency during the collapse period is low. If the potential seismic moment, sometimes called geodetic moment, is estimated from the definition $\mathbf{M}_G = \mu \underline{\mathbf{u}} \mathbf{A}$ and assumed all the faulting ($\underline{\mathbf{u}}$) takes place on the caldera boundary fault, a total of 65 m, we get \mathbf{M}_G equal to 1.4×10^{20} Nm. The area of the caldera fault (\mathbf{A}) is estimated from the diameter of the caldera block of 6 km and depth to the brittle-ductile transition of 8 km, both values derived from Guðmundsson *et al.* (2016). A value of 13 GPa is used for the shear modulus (μ) of the brittle crust, following Grapenthin *et al.* (2006) and assuming the shear modulus is one third of the Young's modulus. The released seismic moment of all earthquakes during the collapse (\mathbf{M}_0), on the other hand, is 9.3×10^{18} Nm, a factor of 15 lower. Here we use $\mathbf{M} = 2/3 \log \mathbf{M}_0 - 6.0$ to convert magnitude to seismic moment. The seismic efficiency or moment ratio $\mathbf{M}_0/\mathbf{M}_G$ is 0.066 and falls within the range of values for magmatically controlled events (e.g. Pedersen *et al.*, 2007). It is thus clear that a substantial part of the fault displacement takes place by aseismic creep. The same conclusion may be drawn from the fact that the hypocenters are unevenly distributed along the ring fault. The earthquakes line up along the northern and southern sections of the fault, whereas the eastern and western parts are almost devoid of earthquake sources (Figure 1). It is therefore conceivable that different sections of the fault react very differently to the high strain rate at the boundaries of the caldera block.

The deviation from the linear relationship of the Gutenberg-Richter equation becomes extreme in the case of the caldera earthquakes during the collapse period. As we show, the magnitude-frequency distribution of these earthquakes can be modeled as the sum of two populations, population A of small earth-

quakes, which behaves like the Gutenberg-Richter equation prescribes, and population B of larger events which can be modeled with a normal distribution. This is by no means a unique model of the over-all distribution, but calls for some speculation on possible explanations. We note that these events take place during very unusual circumstances, in a limited volume of rock, bounded by a circular fault, and under very high strain rate. Most of the earthquakes take place on the boundary fault, as seen in Figure 1. The block was subsiding at a fairly steady rate as high as half a meter per day. One may argue that the dimension of the source faults of the population A earthquakes was well within the dimension of the caldera block and to them the faulted volume was like any other infinite, seismically active volume of rock, hence in accord with the Gutenberg-Richter relation. The earthquakes of population B were larger, however, and involved a good part of the circular caldera fault where different size limitations are in effect. There may be a characteristic earthquake, the magnitude of which may be determined by the circumference of the caldera and the subsidence rate of the caldera floor. We note, for example, that the magnitude of these earthquakes appears to decrease as the collapse continues and the subsidence rate decreases (Figure 5). The source dimension of the events of population B may be estimated, for example, by applying the source scaling relationships of Abercrombie (1995). An earthquake of magnitude 4 would have a source dimension of 160 m -1600 m, depending on the assumed stress drop, varying between 100 MPa and 0.1 MPa, respectively. The corresponding values for a magnitude 5 event would be 500 m – 5000 m. Considering the volcanic environment and the low seismic efficiency one may argue that the stress drop is more likely to be on the low side, and therefore the source dimensions on the high side.

It may be of some importance for monitoring purposes to determine when the magnitude distribution in a remote caldera becomes bi-modal as in the case of Bárðarbunga. The statistical problem of detection is worth a special study and is outside of the scope of this paper. We point out, however, that the earthquakes exceeding magnitude 5 began four days into

the deflation period of Bárðarbunga (Gudmundsson *et al.*, 2016), when the deflation had reached the limit to activate the caldera fault. They then continued for the remaining time of the collapse and eruption. These large events make up the bulk of the population B events.

Greenfield *et al.* (2018) report a study of the seismicity of the Askja and Bárðarbunga volcanoes, including a study of the b-value of Bárðarbunga caldera earthquakes. They ran a network of up to 70 seismographs around these volcanoes, beginning in 2008. Their catalog of Bárðarbunga earthquakes was continuous between January 2013 and the end of 2015, i.e. only a part of our study period. On the other hand, their catalog includes earthquakes of smaller magnitude. In general, their b-values are higher than the ones reported here for the periods where the studies overlap. For the period before the collapse, 2013 to July 2014, they determine a rather stable b-value of 1.2-1.4, whereas our value is around 0.9, also quite stable. They report a drop in the b-value during the collapse, but do not note the severe deviation from linearity in the magnitude distribution. In the post-collapse period, March-December 2015, both studies show variable b-values, beginning at 1.3-1.5 and decreasing with time. The systematic difference between the results of the two studies may be caused by the different methods to determine the b-value. In the study of Greenfield *et al.* (2018) it is assumed that the distribution is linear. In our study we try to account for the apparent deviation from linearity by fitting three line segments to the magnitude distribution. Our b-value is then determined from the slope of the middle segment, that always has a smaller average slope than the whole curve.

The reasons for temporal changes in b-value in the caldera area are not likely to be found in structural differences. There was no significant change in the spatial distribution of the hypocenters during the period of study while the b-value changed. Instead, we suggest that the changes are due to temporal variations in stress in the hypocentral volume at Bárðarbunga caldera. Slight inflation was detected in the volcano prior to the failure of the magma chamber wall in August 2014 (Sigmundsson *et al.*, 2015).

The high b-value and low seismicity following the collapse of the caldera is consistent with low stress above a deflated magma chamber. The increase in seismicity in the post-collapse period concurs with results of GPS-measurements in the region around the volcano that show re-inflation (Sigmundsson *et al.*, 2018). The drop in b-value is also consistent with increasing stress in the caldera region.

Geodetic methods in conjunction with seismicity have proved very successful for the monitoring of activity of Icelandic volcanoes (e.g., Sturkell *et al.*, 2006; Sigmundsson *et al.*, 2018; Einarsson, 2018). One of the main obstacles, however, is the glacier coverage of some of the most active volcanoes, such as Katla, Grímsvötn, and Bárðarbunga, that limits the usefulness of geodetic methods. Geodetic stations have to be located on nunataks or bedrock sites outside the glacier, which usually means that they are at considerable distance from the center of pressure variation within the volcano. We have here documented a case where the b-value of caldera earthquakes varies systematically with expected pressure variations. The correlation between the two therefore may be diagnostic, and both can be used as stress indicators. The relationship might be calibrated on a suitably located volcano using GPS measurements of inflation and the analysis of stress perturbations around a magmatic system, e.g. by Albino *et al.* (2010), to constrain better the failure limit of a magma chamber. The b-value may thus add to the set of parameters for volcano monitoring and may be particularly useful for subglacial volcanoes where other methods are difficult.

CONCLUSIONS

1. The b-value of caldera earthquakes associated with the ongoing activity of the Bárðarbunga volcano shows systematic variations that appear to reflect physical processes in the caldera.
2. In the period preceding the rupture of the caldera wall in August 2014 the seismicity of the caldera was moderate. The b-value was 0.83 for the period 2010 until the magma chamber wall ruptured and a lateral dike propagated away from the caldera.
3. Earthquakes associated with the subsequent slow collapse of the caldera in response to the dike prop-

agation and eruption from its distal end show an unusual magnitude distribution that does not conform to the Gutenberg-Richter power law. The earthquake sequence may be described as consisting of two populations, one with a typical magnitude distribution according to the Gutenberg-Richter relationship, the other with a normal distribution with a peak at M about 4.

4. The seismic activity reached a low following the end of the eruption and the collapse of the caldera in February 2015. The b -value took a typical value around 1.2. Several months later the activity increased significantly and reached a constant moment release rate. The b -value decreased to 0.4. The constant seismicity and lowered b -value is consistent with increasing stress caused by re-inflation of the volcano, as shown by deformation measurements.

Acknowledgements

Seismicity data are from the website of the Icelandic Meteorological Office, www.vedur.is. Ásta Rut Hjartardóttir made Figure 1. Funding from the Icelandic Students Innovation Fund is acknowledged. The manuscript benefitted greatly from three anonymous reviews.

ÁGRIP

Stærðardreifingu jarðskjálfta á tilteknu svæði og tímabili er oft lýst með formúlu sem kennd er við Gutenberg og Richter, $\log N = a - bM$. N er þá fjöldi skjálfta af stærðinni M og stærri, a og b eru fastar. Fyrri fastinn, a , segir til um fjölda skjálfta af stærðinni 0 og stærri, b -gildið segir hins vegar til um hvernig hlutfalli stórra skjálfta á móti minni skjálftum er háttad, og er oft talið vera háð ástandi svæðisins eða spennunni í jarðskorpunni. Oftast er b nálægt 1 og breytist lítið. Hátt b -gildi er talið tengjast lágri bergspennu og lágt b -gildi hárrí. Við könnun á stærðardreifingu skjálfta í öskju Bárðarbungu kemur í ljós að b -gildi þeirra breytist talsvert og virðist breytingin vera í samræmi við það sem búast má við í sambandi við umbrot þau sem þar hafa verið undanfarnin ár. Breytingin er sérstaklega áberandi eftir að eldgosinu í Holuhrauni lauk í febrúar 2015 og sigið mikla í öskju Bárðarbungu hætti. Í fyrstu var b -gildið hátt sem benti til þess að spenna væri lág í berginu innan

öskjunnar. Á sama tíma var jarðskjálftavirkni fremur lítil. Í lok ársins 2015 tók skjálftavirkni innan öskjunnar að vaxa og jafnframt lækkaði b -gildið. Hvort tveggja bendir til hækkandi spennu yfir kvikuhólfinu undir öskjunni. Mælingar á aflögun jarðskorpunnar umhverfis eldstöðina benda til þess að hún hafi þanist út á sama tíma. Ákvarðanir á b -gildi skjálftavirkninnar á undan gosinu eru ekki eins áreiðanlegar. Skjálftavirknin var fremur hófleg og b -gildi hennar var 0.83, áður en kvikuhólfið brast 16. ágúst 2014 og kvikugangurinn skaust norður í Holuhraun þar sem hann náði yfirborði og fóðraði eldgosid. Jarðskjálftavirknin í öskjunni jókst mjög meðan á gosinu stóð og öskjubotninn hrundi um 65 metra á sex mánuðum. Stærðardreifing skjálftanna á þessu tímabili var með mjög óvenjulegum hætti. Hún fellur ekki vel að lögmáli Gutenbergs og Richters. Herma má dreifinguna með tveimur skjálftarunum, þar sem önnur sýnir venjulega stærðardreifingu en hin inniheldur skjálfta af stærð sem má lýsa með normaldreifingu með meðalgildi nálægt 4. Þessar niðurstöður benda til þess að stærðardreifing jarðskjálfta gefi uppýsingar um ástand eldstöðvar og megi því nota við mat á eldgosahættu ásamt öðrum mælingum. Það getur skipt máli, sérstaklega þegar í hlut eiga eldstöðvar sem eru huldar jökli og því erfitt að koma við öðrum mælingum.

REFERENCES

- Abercrombie, R.E. 1995. Earthquake source scaling relationships from -1 to 5 M_L using seismograms recorded at 2.5 km depth. *J. Geophys. Res.* 100, 24,015–24,036.
- Ágústsdóttir, Th., T. Winder, J. Woods, R.S. White, T. Greenfield and B. Brandsdóttir 2019. Intense seismicity during the 2014–2015 Bárðarbunga-Holuhraun rifting event, Iceland, reveals the nature of dike-induced earthquakes and caldera collapse mechanisms. *J. Geophys. Res. Solid Earth* 124, 8331–8357. <https://doi.org/10.1029/2018JB016010>
- Albino, F., V. Pinel and F. Sigmundsson 2010. Influence of surface load variations on eruption likelihood: application to two Icelandic subglacial volcanoes, Grímsvötn and Katla. *Geophys. J. Int.* 181, 1510–1524. <https://doi.org/10.1111/j.1365-246X.2010.04603.x>
- Bjarnason, I.Th. 2014. The 1973–1996 earthquake sequence in Bárðarbunga volcano: Seismic activity lead-

- ing up to eruptions in NW-Vatnajökull. *Jökull* 64, 61–82.
- Björnsson, H. 1988. Hydrology of Ice Caps in Volcanic Regions. *Soc. Sci. Isl.* 45, Reykjavík, 139 pp.
- Björnsson, H. and P. Einarsson 1990. Volcanoes beneath Vatnajökull, Iceland: Evidence from radio-echo sounding, earthquakes and jökulhlaups. *Jökull* 40, 147–168.
- Einarsson, P. 1986. Seismicity along the eastern margin of the North American Plate. In: Vogt, P.R. and B.E. Tucholke (eds.), *The Geology of North America, Vol. M, The Western North Atlantic Region*. Geological Society of America, 99–116.
- Einarsson, P. 1991a. Earthquakes and present-day tectonism in Iceland. *Tectonophysics* 189, 261–279.
- Einarsson, P. 1991b. Umbrotin við Kröflu 1975–1989 (The activity of Krafla 1975–1989, in Icelandic). In: Einarsson, Á., and A. Garðarsson (eds.). *Náttúra Mývatns. Hið Íslenska Náttúrufræðifélag*, 97–139.
- Einarsson, P. 2008. Plate boundaries, rifts and transforms in Iceland. *Jökull* 58, 35–58.
- Einarsson, P. 2018. Short-term seismic precursors to Icelandic eruptions 1973–2014. *Frontiers in Earth Science* 6:45. <https://doi.org/10.3389/feart.2018.00045>
- Einarsson, P. and S. Björnsson 1987. Seismological measurements at the Science Institute, University of Iceland. In: Sigfússon, Þ.I. (ed.). *Í hlutarins eðli*, Festschrift for Þorbjörn Sigurgeirsson. Menningarsjóður, Reykjavík, 251–278.
- Einarsson, P. and K. Sæmundsson 1987. Earthquake epicentres 1982–1985 and volcanic systems in Iceland: A map in: Sigfússon, Þ.I. (ed.). *Í hlutarins eðli*, Festschrift for Þorbjörn Sigurgeirsson. Menningarsjóður, Reykjavík.
- Einarsson, P., B. Brandsdóttir, M.T. Guðmundsson, H. Björnsson, K. Grönvold and F. Sigmundsson 1997. Center of the Iceland hotspot experiences volcanic unrest. *Eos Transactions* 78, no. 35, 369, 374–375.
- El-Isa, Z.H. and D.W. Eaton 2014. Spatiotemporal variations in the *b*-value of earthquake magnitude-frequency distributions: Classification and causes. *Tectonophysics* 615–616, 1–11. <https://doi.org/10.1016/j.tecto.2013.12.001>
- Grapenthin, R., F. Sigmundsson, H. Geirsson, Th. Árnadóttir and V. Pinel 2006. Icelandic rhythmicity: Annual modulation of land elevation and plate spreading by snow load. *Geophys. Res. Lett.* 33, L24305, <https://doi.org/10.1029/2006GL028081>
- Greenfield, T., R.S. White, T. Winder and Th. Ágústsdóttir 2018. Seismicity of the Askja and Bárðarbunga volcanic systems of Iceland, 2009–2015. *J. Volc. Geothermal Res.* <https://doi.org/10.1016/j.jvolgeores.2018.08.010>
- Guðmundsson, M.T., F. Sigmundsson and H. Björnsson 1997. Ice-volcano interaction of the 1996 Gjalp subglacial eruption, Vatnajökull, Iceland. *Nature* 389, 954–957.
- Guðmundsson, M.T., K. Jónsdóttir, A. Hooper, E.P. Holohan, S.A. Halldórsson, B.G. Ófeigsson, S. Cesca, K.S. Vogfjörð, F. Sigmundsson, Th. Högnadóttir, P. Einarsson, O. Sigmarsson, A.H. Jarosch, K. Jónasson, E. Magnússon, S. Hreinsdóttir, M. Bagnardi, M. Parks, V. Hjörleifsdóttir, F. Pálsson, T. R. Walter, M.P.J. Schöpfer, S. Heimann, H.I. Reynolds, S. Dumont, E. Bali, G.H. Gudfinnsson, T. Dahm, M. Roberts, M. Hensch, J.M.C. Belart, K. Spaans, S. Jakobsson, G.B. Guðmundsson, H.M. Fridriksdóttir, V. Drouin, T. Dürig, G. Adalgeirsdóttir, M.S. Rishuus, G.B.M. Pedersen and T. van Boeckel 2016. Gradual caldera collapse at Bárðarbunga volcano, Iceland, regulated by lateral magma outflow. *Science* aaf8988. <https://doi.org/10.1126/science.aaf8988>
- Heimisson, E.R., P. Einarsson, F. Sigmundsson and B. Brandsdóttir 2015. Kilometer-scale Kaiser effect identified in Krafla volcano, Iceland. *Geophys. Res. Lett.* 42, <https://doi.org/10.1002/2015GL065680>
- Hjartardóttir, Á.R., P. Einarsson, S. Magnúsdóttir, Þ. Björnsdóttir and B. Brandsdóttir 2016a. Fracture systems of the Northern Volcanic Rift Zone, Iceland. – An onshore part of the Mid-Atlantic plate boundary. In: Wright, T.J., A. Ayele, D.J. Ferguson, T. Kidane and C. Vye-Brown (eds.). *Magmatic Rifting and Active Volcanism*. Geological Society, London, Special Publications, 420, <http://dx.doi.org/10.1144/SP420.1>
- Hjartardóttir, Á.R., P. Einarsson, M.T. Guðmundsson and Th. Högnadóttir 2016b. Fracture movements and graben subsidence during the 2014 Bárðarbunga dike intrusion in Iceland. *J. Volc. Geothermal Res.* 310, <https://doi.org/10.1016/j.jvolgeores.2015.12.002>
- Hjartarson, Á. 1994. Environmental changes in Iceland following the Great Þjórsá Lava Eruption 7800 14C years BP. In: Stötter, J. and F. Wilhelm (eds.). *Environmental Change in Iceland*, München, 147–155.
- Hjartarson, Á. and K. Sæmundsson 2014. *Bedrock map of Iceland in 1:600 000*. ÍSOR, Reykjavík.
- Jakobsdóttir, S.S. 2008. Seismicity in Iceland: 1994–2007. *Jökull* 58, 75–100.

- Kulhanek, O. 2005. *Seminar on b-value*. Charles University, Prague, Dept. of Geophysics, Dec. 10–19.
- Larsen, G. 1984. Recent volcanic history of the Veidivötn fissure swarm, southern Iceland – an approach to volcanic risk assessment. *J. Volc. Geothermal Res.* 22, 33–58.
- Muggeo, V.M.R. 2003. Estimating regression models with unknown break-point. *Statistics in Medicine* 22, 3055–3071. <https://doi.org/10.1002/sim.1545>
- Nettles, M. and G. Ekström 1998. Faulting mechanism of anomalous earthquakes near Bárðarbunga Volcano, Iceland. *J. Geophys. Res.* 103, 17,973–17,983.
- Pedersen, R., F. Sigmundsson and P. Einarsson 2007. Controlling factors on earthquake swarms associated with magmatic intrusions; constraints from Iceland. *J. Volc. Geothermal Res.* 162, 73–80, <https://doi.org/10.1016/j.jvolgeores.2006.12.010>
- Riedel, C., T. Petersen, F. Theilen and S. Neben 2003. High b-values in the leaky segment of the Tjörnes Fracture Zone north of Iceland: are they evidence for shallow magmatic heat sources? *J. Volc. Geothermal Res.* 128, 15–29.
- Scholz, C. 1968. The frequency-magnitude relation of microfracturing in rock and its relation to earthquakes. *Bull. Seismol. Soc. Am.* 58, 399–415.
- Sigmundsson, F., A. Hooper, S. Hreinsdóttir, K.S. Vogfjörð, B.G. Ófeigsson, E.R. Heimisson, S. Dumont, M. Parks, K. Spaans, G.B. Guðmundsson, V. Drouin, T. Árnadóttir, K. Jónsdóttir, M.T. Guðmundsson, T. Högnadóttir, H.M. Fridriksdóttir, M. Hensch, P. Einarsson, E. Magnússon, S. Samsonov, B. Brandsdóttir, R.S. White, T. Ágústsdóttir, T. Greenfield, R.G. Green, Á.R. Hjartardóttir, R. Pedersen, R.A. Bennett, H. Geirsson, P.C. La Femina, H. Björnsson, F. Pálsson, E. Sturkell, C.J. Been, M. Möllhoff, A.K. Braidon and E.P.S. Eibl 2015. Segmented lateral dyke growth in a rifting event at Bárðarbunga volcanic system, Iceland. *Nature* 517, 191–195. <https://doi.org/10.1038/nature14111>
- Sigmundsson, F., M. Parks, R. Pedersen, K. Jónsdóttir, B.G. Ófeigsson, R. Grapenthin, S. Dumont, P. Einarsson, V. Drouin, E.R. Heimisson, Á.R. Hjartardóttir, M.T. Guðmundsson, H. Geirsson, S. Hreinsdóttir, E. Sturkell, A. Hooper, P. Högnadóttir, K. Vogfjörð, T. Barnie and M. Roberts 2018. Magma movements in volcano plumbing systems and their associated ground deformation and seismic pattern. Burchardt, S. (ed.), chapter 11 in *Volcanic and Igneous Plumbing Systems*, 285–322, Elsevier. <https://doi.org/10.1016/B978-0-12-809749-6.00011-X>
- Sturkell, E., P. Einarsson, F. Sigmundsson, H. Geirsson, R. Pedersen, E. Van Dalssen, A. Linde, S. Sacks and R. Stefánsson 2006. Volcano geodesy and magma dynamics in Iceland. *J. Volc. Geothermal Res.* 150, 14–34. <https://doi.org/10.1016/j.jvolgeores.2005.07.010>.
- Svavarsdóttir, S.I., S.A. Halldórsson and G.H. Guðfinnsson 2017. Geochemistry and petrology of Holocene lavas in the Bárðardalur region, N-Iceland. Part I: Geochemical constraints on source provenance. *Jökull* 67, 17–42.
- Sykes, L. 1970. Earthquake swarms and sea-floor spreading. *J. Geophys. Res.* 75, 6598–6611.
- Sæmundsson, K. 1978. Fissure swarms and central volcanoes of the neovolcanic zones in Iceland. In: Bowes, D. R. and B.E. Leake (eds.). *Crustal evolution in northwestern Britain and adjacent regions. Geol. J. Special Issue* 10, 415–432.
- Thorarinsson, S., K. Sæmundsson and R.S. Williams 1973. ERTS-1 image of Vatnajökull: Analysis of glaciological, structural, and volcanic features. *Jökull* 23, 7–17.
- Wiemer, S., S.R. McNutt and M. Wyss 1998. Temporal and three-dimensional spatial analyses of the frequency-magnitude distribution near Long Valley Caldera, California. *Geophys. J. Int.* 134, 409–421.
- Wolfe, C.J., I.Th. Bjarnason, J.C. VanDecar and S. Solomon 1997. Seismic structure of the Iceland mantle plume. *Nature* 385, 245–247.
- Wyss, M. 1973. Towards a physical understanding of the earthquake frequency distribution. *Geophys. J. R. astr. Soc.* 31, 341–359.
- Zobin, V.M. 1999. The fault nature of the Ms 5.4 volcanic earthquake preceding the 1996 subglacial eruption of Grimsvötn volcano, Iceland. *J. Volc. Geothermal Res.* 92, 349–358.